Singh and Behera, J Material Sci Eng 2016, 6:1
DOI: 10.4172/2169-0022.1000304

Journal of Material Sciences & Engineering

Research Article Open Access

Prediction of Geometry of Loop Formed on Terry Fabric Surface Using Mathematical and FEM Modelling

Singh JP[1]* and Behera BK[2]

[1]*Department of Textile Technology, U.P.Textile Technology Institute, Kanpur, India*
[2]*Department of Textile Technology, Indian Institute of Technology Delhi, New Delhi, India*

Abstract

The objective of this study is to understand the loop formation phenomenon of yarn by considering their non-linear bending behaviour and the effect of loop shape factor on properties of terry fabric. The yarn is modelled as a continuum thin solid beam, and the governing buckling equation is derived using Timoshenko's elastic theory and the Bernoulli-Euler theorem. Since the formation of loop is effected by large deformation caused by the weight of yarn too, geometric non-linearity is also considered and Runge Kutta method of numerical technique is used to solve the governing equation. Further, finite element modelling technique is also used to see the accuracy of the prediction which is further verified by the actual experimental results. The results of the research prove that the finer yarn produce loops which are having more circularity i.e., higher loop shape factor, as compared to the loops produced from coarse yarn. It is also being proved that the increasing the loop length increases circularity of the loop i.e., higher loop shape factor.

Keywords: Loop geometry; Terry fabric; Non-linear material; Numerical analysis; Finite element simulation

Introduction

The functional and aesthetic characteristics of terry fabric are predominantly governed by the geometrical profile of the loop [1-3]. The geometrical configuration of loop is primarily determined by yarn characteristics. Substantial amount of research work has been carried out to reveals the relationship between yarn properties and fabric properties. Loop geometry which is the peculiarity of the terry fabric has been ignored by most researchers. It seems to be interesting to know the relation between yarn properties and loop geometry.

Formation of loop on fabric surface is effected by buckling of yarn which is largely influenced by its bending behaviour. The yarn bending rigidity can be evaluated experimentally by defining it as a Bernoulli-Euler beam and differentiating the moment curvature relationship. Similar to the fabric, in the early stage of yarn bending process, a higher moment to overcome the interfibre friction is required to bend the unit curvature, and then after less moment is need for further bending. In both friction couple theory [4-7] and bilinear model [8,9] this early stage phenomenon is neglected, assuming a linear moment curvature relationship. In some latest research moment-curvature relationship was explained by an exponential function [10,11]. Therefore, we considered yarn bending as a highly non-linear phenomenon without any assumption [12,13].

The objective of this study is to understand the loop formation phenomenon of yarn by considering their non-linear bending behaviour. The yarn is modelled as a continuum thin solid beam, and the governing buckling equation is derived using Timoshenko's elastic theory and the Bernoulli-Euler theorem. Since the formation of loop is effected by large deformation caused by the weight of yarn too, geometric non-linearity is also considered and Runge Kutta method of numerical technique is used to solve the governing equation. Further, FEM modelling technique is also used to see the accuracy of the prediction which is further verified by the actual experimental results.

Formation of Loop during Terry Weaving

Formation of terry loop during terry weaving (Figure 1) is a process of buckling. Buckling is a mode of failure in which the structure experiences sudden failure when subjected to a compressive stress. During formation of loop, the structural behaviour has been found markedly non-proportional to the applied load which suggests the high non-linearity of the system of loop formation. These nonlinearities have to be considered to obtain the correct solution. Instead of one step solution found in linear problems, the non-linear problem is solved by incremental method [14,15].

Loop Shape Factor

Aspect ratio and shape factor are two important quantities that explain the geometry of any shape. Aspect ratio is the ratio of major

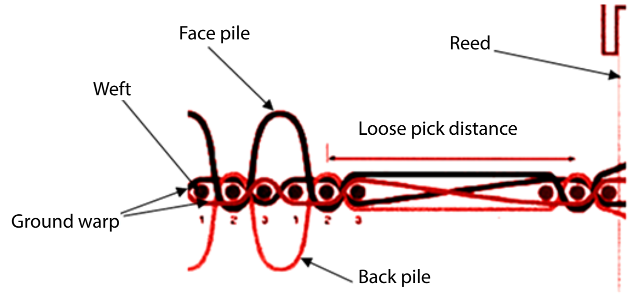

Figure 1: Loop formation showing the yarn segment between fell of cloth and reed.

***Corresponding author:** Singh JP, Department of Textile Technology, UP Textile Technology Institute, Kanpur, India, Tel: 05122531814; E-mail: jpsingh.iitd@gmail.com

Received November 10, 2016; **Accepted** November 21, 2016; **Published** November 30, 2016

Citation: Singh JP, Behera BK (2016) Prediction of Geometry of Loop Formed on Terry Fabric Surface Using Mathematical and FEM Modelling. J Material Sci Eng 6: 304. doi: 10.4172/2169-0022.1000304

axis length to the minor axis length. It is suitable for the regular shapes while shape factor is suitable for all kind of shapes. Loop shape factor is a measure of circularity of loop. Here loop shape factor is calculated as shown below.

Loop shape factor=loop area/perimeter of the loop

=loop area/(*l*+*d*)

Where *l*=loop length, *d*=distance between two legs (Figure 2).

Theoretical Analysis

Loop geometry has been described here by the loop shape factor. Loop shape factor is a measure of circularity of the terry pile loop which is defined as the ratio of maximum loop height to the maximum loop width.

Mathematical modelling

Using KES-FB2 bending tester, moment curvature relationships and consequently regression equation (1) were obtained:

$$m(k) = c_0\ k + c_1\left\{1 - e^{-\acute{a}k}\right\} \tag{1}$$

where m=moment, k=curvature, and c_0, c_1, β are constants having a value of 0.024, 0.015, and 2.89, respectively.

The yarn bending properties were successfully modelled here using exponential function giving standard error compared to the KES-FB2 m-k relationship below 0.002 and R^2 higher than 0.96. Differentiating Equation (1) gives the bending rigidity- curvature relationship, Equation (2):

$$b(k) = c_0 + \beta c_1 e^{-\beta k} \tag{2}$$

where b=bending rigidity, k=curvature, and c_0, c_1, β are constants. Equation is plotted in Figure 3 for 100% cotton yarn, which shows that the bending rigidity is non-linear in nature.

Mathematical model and governing equation: According to large deformation beam theory, the curvature for a large deformation problem can be defined as:

$$k = \frac{d\theta}{ds} \tag{3}$$

Where θ = tangent angle at some point of the beam, s = arc length.

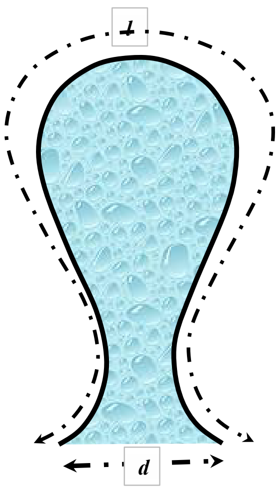

Figure 2: Loop geometry.

According to elastic beam theory bending rigidity can be expressed as b (k). So Bernoulli-Euler theory for m-k relationship can be expressed as:

$$\frac{d\theta}{ds} = \frac{m}{b(k)} \tag{4}$$

Elastica model and governing equation: Yarn had been modelled after Timoshenko's elastic assuming it as bent bean with an identical cross-section. The moment equilibrium of the elastic model shown in Figure 4, gives the governing Equation (5).

$$b(k)\frac{d\theta}{ds} = b(s)\frac{d\theta}{ds} = -Py + me + Rx - \int_0^s w(x - x')ds' \tag{5}$$

Where P=compression load applied at the ends of beam, R=reactive force for the weight of beam, me= external moment, w=weight per unit length.

Differentiating Equation (5) by gives

$$b_d(s)\frac{d^2\theta}{ds^2} = -Psin\theta + (R - ws)cos\theta \tag{6}$$

Where:

$$b_d(s) = \left\{c_0 + \beta c_1\left(1 - \beta\frac{d\theta}{ds}\right)exp\left(-\beta\frac{d\theta}{ds}\right)\right\} \tag{7}$$

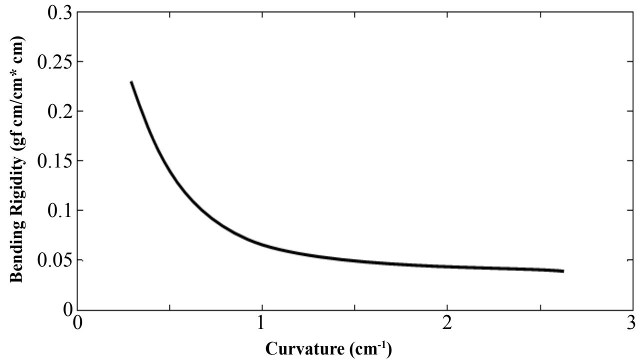

Figure 3: Relationship between bending rigidity and curvature of yarn.

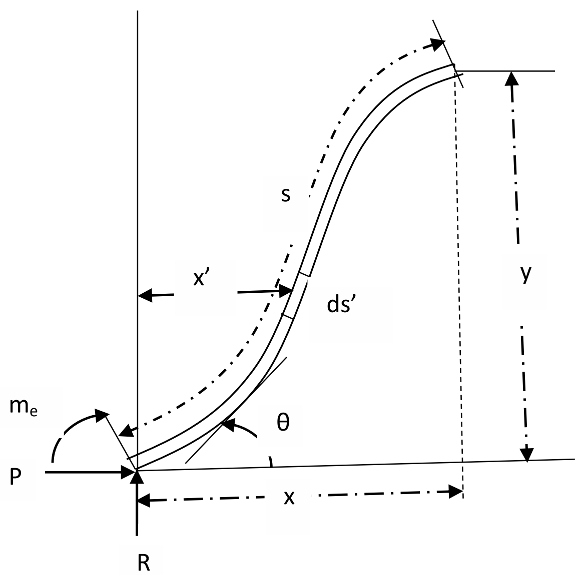

Figure 4: Yarn Elastic loop model.

Numerical analysis: Highly non-linear differential Equation (6) can be solved by fourth-order Runge-Kutta method. The second order governing equation is modified into a system of two first order equations and normalised as in Equation (7):

$$\frac{d\theta}{d\bar{s}} = \varphi \quad (7a)$$

$$\frac{d\varphi}{d\bar{s}} = -\bar{P}sin\theta + \left(\bar{R} - \bar{W}\bar{s}\right)cos\theta \quad (7b)$$

Formation of yarn loop which is governed by the highly nonlinear differential Equation (7) is a two point boundary problem which can be effectively solved by shooting method considering the following condition.

$$0 \le \bar{s} \le 1 \quad (8a)$$

$$\theta|_{\bar{s}=0,0.5,1} = 0 \quad (8b)$$

$$\bar{R} = 0.5\bar{W} \quad (8c)$$

Finite element modelling

The functional and aesthetic characteristics of terry fabric are predominantly governed by the geometrical profile of the loop. The geometrical configuration of loop is primarily determined by yarn characteristics. Need of precise study on how the yarn properties control the geometrical profile of the loop motivated us to explore the outcome using FEM.

According to principle of virtual work, it possible to represent the distributed displacement field $\{u\}$ of any solid body by

$$\{u\} = [N]\{r\} \quad (9)$$

where $[N]$=set of known function of coordinates; $\{r\}$=set of constants

It follows that the algebraic equations for the axially loaded bar analysis are of the form

$$[K]\{r\} = \{R\} \quad (10)$$

Where $[K]$=stiffness matrix; $\{r\}$= nodal displacement; $\{R\}$=equivalent nodal loads

The expression for $[K^d]$ supposes that N is known. In the case of simple beams with a single axial load at one end, we have N= − P and

$$\left[K^d\right]\{r\} = -P\int [N']^T [N']\{r\}dx \quad (11)$$

Adding shape function (equation 3) to equation 2

$$\left([K] + \left[K^d\right]\right)\{r\} = \{R\} \quad (12)$$

Where $[K^d]$=differential stiffness;

$$[K] = \int\left[B^T\right][G][B]dv = \int EI[N'']^T[N'']dx$$

$$[R] = \int[N]^T f(x)dx + \sum\left[\left[N(x_i)\right]^T F_{Zi} + W\left[N'(x)_j\right]^T M_{yj}\right]$$

Equation (12) is a matrix equation for a beam- column. In case of buckling

$$\left([K] + \left[K^d\right]\right)\{r\} = \{0\}$$

Subsequently, critical load can be found by setting:

$$\left|[K] - P\left[K^d\right]\right| = 0 \quad (13)$$

Expanding the determinant in Equation (13) will produce a polynomial in P and the lowest root of this polynomial is critical value of P. For large deformation we take shape function as:

$$[n] = \frac{1}{L^3}\left[L^3 - 3L^2 s + 2s^3,\ L^3 s - 2L^2 s^2 + Ls^3, 3Ls^2 - 2s^3, -L^2 s^2 + Ls^3\right] \quad (14)$$

Where L= length of element, s=distance measured from a node at one end of the element and is positive in the direction of the other node. The element stiffness matrix is:

$$[K_i] = \frac{EI}{L_i^3}\begin{bmatrix} 12 & -6L_i & -12 & -6L_i \\ -6L_i & 4L_i^2 & 6L_i & 2L_i^2 \\ -12 & 6L_i & 12 & 6L_i \\ -6L_i & 2L_i^2 & 6L_i & 4L_i^2 \end{bmatrix} \quad (15)$$

Inserting shape function into the integral for the element differential stiffness matrix gives us--

$$[K^D]_i = \int_0^{L_i}[n']_i^T[n]_i ds \frac{1}{30L_i}\begin{bmatrix} 36 & -3L_i & -36 & -3L_i \\ -3L_i & 4L_i^2 & 3L_i & L_i^2 \\ -36 & 3L_i & 36 & 3L_i \\ -3L_i & -L_i^2 & 3L_i & 4L_i^2 \end{bmatrix} \quad (16)$$

Yarn model: Yarn path and cross- section for designing yarn model, its path is represented by the yarn centre line in three dimensional spaces. SolidWorks 2010 software package is used to build the model. The yarn cross-section is a 2D shape of the yarn when cut by a plane perpendicular to the yarn path tangent. The yarns are treated as solid volumes with circular cross-section. So a circle is swept along the pre designed yarn path to build the yarn geometry. The final outcome is a bend elastica. The bend elastica (Figure 5) is the true representation of the yarn segment between cloth fell and the reed as this yarn segment is in bend condition. Keeping the same spline for the path of the yarn different yarn model has been created by changing the circle diameter for different count of yarn.

Material model: Yarns are modelled as continuum solid bent beam with identical cross-section. The yarn is treated as a non-linear orthotropic material. The longitudinal direction is defined by 11, which is parallel to fibres; the transverse plane is described by the directions 22 and 33, which are characterized by a plane of isotropy at every point in the material. The orthotropic behaviour of the yarn is typically described using a 3D stiffness matrix containing nine independent constants [16]. Since the yarn is transversally isotropic, $E_{22}=_{33}$, υ_{12}-υ_{13} and $G_{12}=G_{13}$. The longitudinal modulus E_{11} is approximated as a linear function of fibre volume fraction V_f of a yarn and fibre modulus E_f by the following equation:

$$E_{11} = \frac{E_f}{V_f} \quad (17)$$

It is assumed that all fibres within a yarn are perfectly parallel and hence no stiffening of the yarn will occur due to fibre straightening at low strains. For simplicity a constant E_{11} ($E_{11}=E_f/V_{f0}$, V_{f0} is initial fibre volume fraction of the yarn) was used in the simulations.

The transverse stiffness, E_{33} ($E_{22}=E_{33}$) can be expressed as a function of strain to express the nonlinearity of the material because the material matrix is no longer constant [17]. The transverse stiffness reduces during the loop formation as the gap between fibres increases.

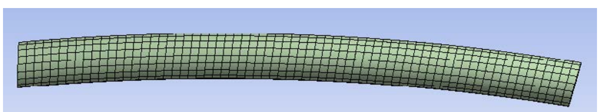

Figure 5: Yarn segment modelled for simulation.

Citation: Singh JP, Behera BK (2016) Prediction of Geometry of Loop Formed on Terry Fabric Surface Using Mathematical and FEM Modelling. J Material Sci Eng 6: 304. doi: 10.4172/2169-0022.1000304

$$E_{33}(\varepsilon_{33}) = \frac{\sigma_{33}}{\varepsilon_{33}} = \frac{-a\left(\frac{V_{f0}}{e^{\varepsilon_{33}}}\right)^{b} + a\left(V_{f0}\right)^{b}}{\varepsilon_{33}} \quad (18)$$

The initial value of E_{33} is

$$E_{33}(0) = \lim_{\varepsilon_T \to 0} \frac{\sigma_T}{\varepsilon_T} = \frac{d\sigma_T}{d\varepsilon_T} = ab\left(\frac{V_{f0}}{e^{\varepsilon_{33}}}\right)^{b} \quad (19)$$

Where V_{f0} is initial fibre volume fraction; $a = 1151$, $b = 12.24$

Due to transverse isotropy, the transverse shear behaviour is characterizes by [18]:

$$G_{23} = \frac{E_{33}}{2(1+\nu_{23})} \quad (20)$$

Material property used for simulation are E_{11} (MPa)=390, E_{33} (MPa)=0.75, G_{12} (MPa)=0.2, G_{23} (MPa)=3.13, ν_{12}=0.32, ν_{23} =0.32, density (kg/m^3) =1530.

FE implementation: According to the proposed algorithm yarn structure model was constructed. The Solidworks 2010 and Ansys 14 software package were used to model the yarn and predict the behaviour and loop shape factor. The yarn was discredited using solid-45, 4-noded tetrahedral three-dimensional elements.

Boundary condition: Keeping yarn length 15 mm constant, yarn diameter varied up to four levels. Fixed support is applied at one end of the yarn, displacement is applied in negative x-direction only (keeping other direction frozen) at the other end. Static structural analysis has been performed keeping large deflection active so that the loop can be formed. In another simulation, yarn length was kept 18 mm and yarn count varied up to two levels.

Actual loop profile

To see the actual loop profile and set up the precise boundary condition for modelling, an experimental setup is done according to Figure 6 which shows the process of loop formation as in actual practice on loom.

Results and Discussion

Loop shape by mathematical modelling

Numerical analysis of the mathematical model gives the loop shape shown in Figure 7 for different weight per unit length/bending rigidity (w/b) ratio. It is clear from Figure 7 that the yarn having lower w/b ratio forms loop of higher shape factor.

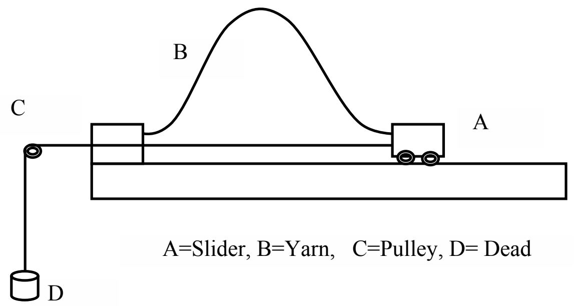

Figure 6: Experimental set up for the process of loop formation.

Loop shape by FEM model

Considering non-linear bending behaviour of yarn i.e., non-linearity in geometrical and bending properties, loop geometry of different yarn count was studied. Results of FEM model were given in the Figures 8-13. These figures the variation in loop shape with the change in yarn count and loop length keeping twist level same. The loop shape factor increases with increase in yarn fineness and this phenomenon is attributed to the reduction in w/b ratio of the yarn.

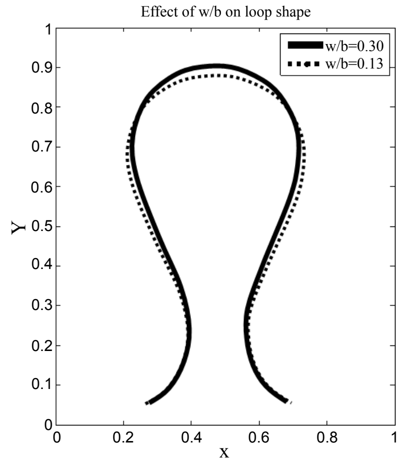

Figure 7: Loop shape by mathematical model.

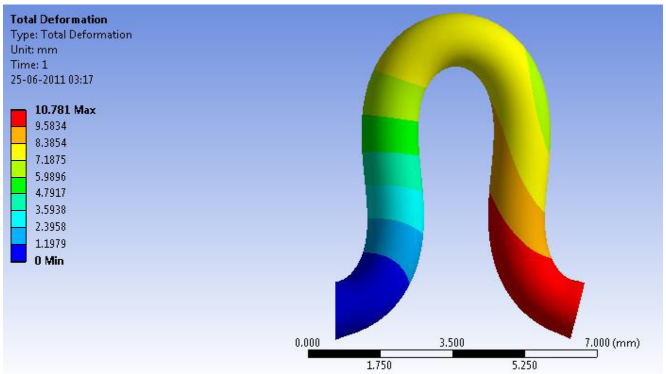

Figure 8: Loop from 6's Ne yarn.

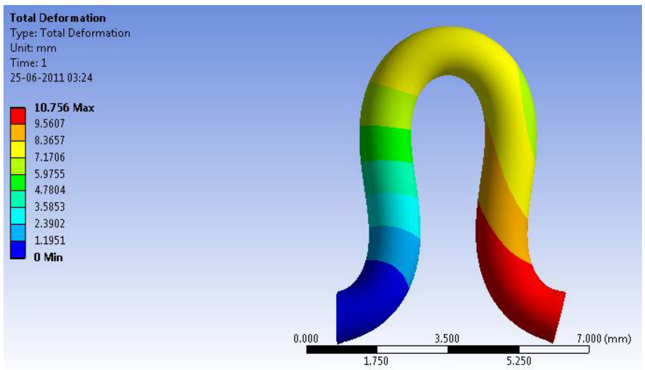

Figure 9: Loop from 8's Ne yarn.

Citation: Singh JP, Behera BK (2016) Prediction of Geometry of Loop Formed on Terry Fabric Surface Using Mathematical and FEM Modelling. J Material Sci Eng 6: 304. doi: 10.4172/2169-0022.1000304

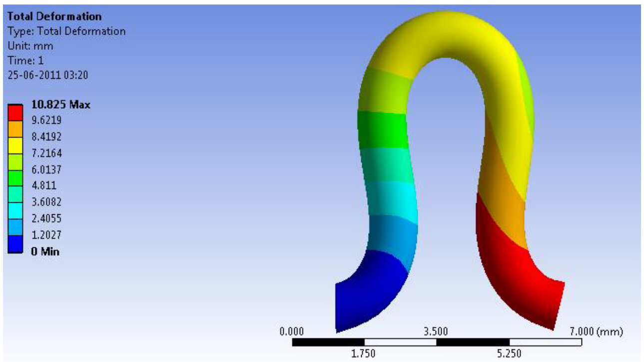

Figure 10: Loop from 12's Ne yarn.

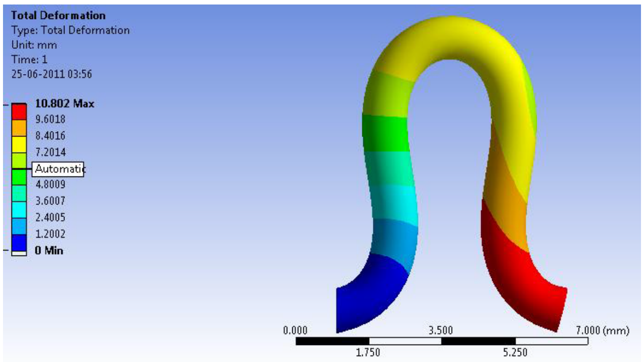

Figure 11: Loop from 14's Ne yarn.

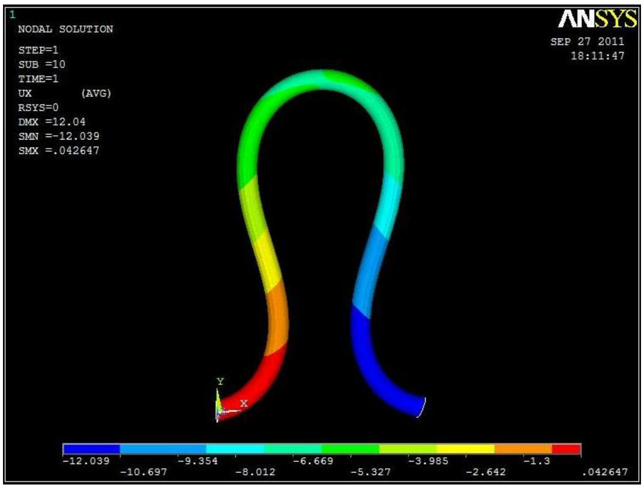

Figure 12: Loop from 14's Ne yarn.

These results are very well supported by the results of our mathematical model as well as earlier research [19,20].

Figures 12 and 13 show the effect of loop length on loop shape factor, the loop shape factor increases with increase in loop length keeping yarn twist level constant.

Actual loop shape

Images of the actual loop shape from different loop length and yarn count produced on the experimental set up has been shown in Figures 14-17. These figures show the similar effect of yarn count and loop length on loop shape factor as the FEM modelled loops.

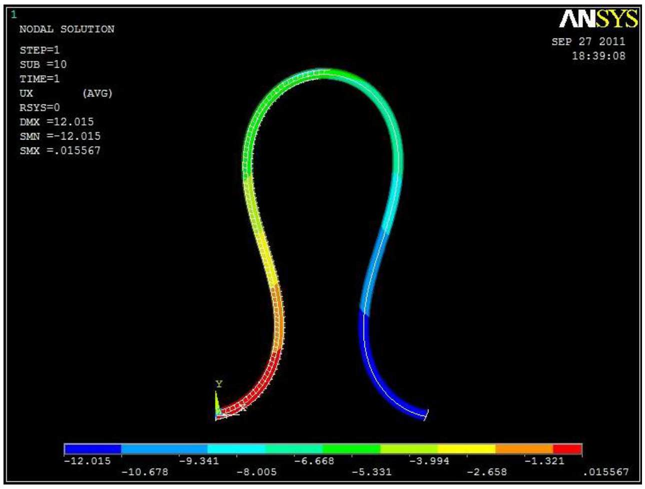

Figure 13: Loop from 20's Ne yarn.

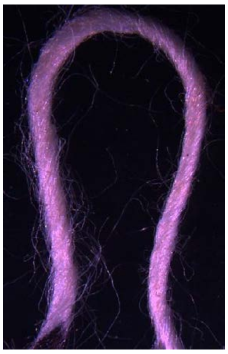

Figure 14: Actual loop from 12's Ne (15 mm).

Figure 15: Actual loop from 14's Ne (15 mm).

Figure 16: Actual loop from 14's Ne (18 mm).

Citation: Singh JP, Behera BK (2016) Prediction of Geometry of Loop Formed on Terry Fabric Surface Using Mathematical and FEM Modelling. J Material Sci Eng 6: 304. doi: 10.4172/2169-0022.1000304

Figure 17: Actual Loop from 20's Ne (18 mm).

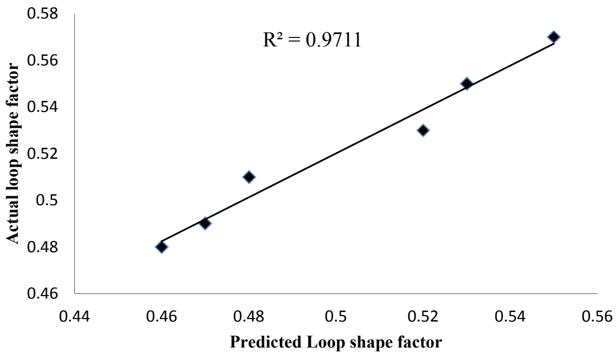

Figure 18: Predicted v/s Experimental loop shape factor.

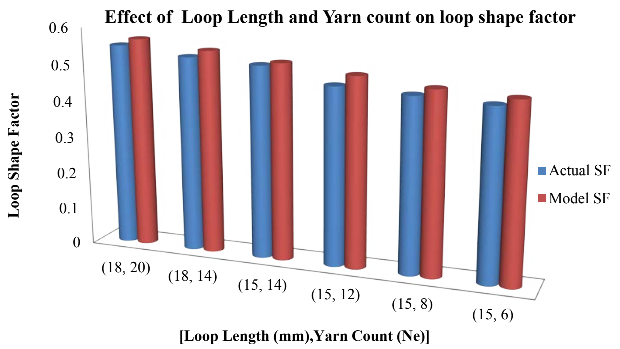

Figure 19: Effect of loop length and yarn count on loop shape factor.

Prediction accuracy of FEM model

Shape factor of the loops and Area under the loop along with the RMSE between predicted and actual results are given in the Table 1. Figure 18 shows that the prediction of loop geometry using finite element method is good which gives R^2 value of 0.951.

Effect of loop length and yarn count on loop shape factor

It is clear from Figure 19 that the loop shape factor affected by loop length and yarn count. Finer yarn and higher loop length gives higher loop shape factor.

Conclusions

Formation of loop on terry fabric surface is affected by buckling of yarn which is highly non-linear. Geometric non-linearity and bending non-linearity both governs the yarn buckling process and consequently the shape of the loop. As mentioned in earlier research, geometric non-linearity is important for modelling large deformation like buckling and non-linear bending rigidity is important to get the real fabric behaviour from model. Considering these two non-linearity, mathematical modelling and finite element modelling was done. Results of FEM model was very well supported by the results of the numerical analysis. Further, the results of FEM model were verified by the actual experimental results and found that the absolute percentage error is 3.86 and R^2 is 0.951. The results of the research prove that the finer yarn produce loops which are having more circularity i.e., higher loop shape factor, as compared to the loops produced from coarse yarn. It is also being proved that the increasing the loop length increases circularity of the loop i.e., higher loop shape factor.

Loop Length (mm), Yarn Count (Ne)	Shape Factor (Model)	Shape Factor (Actual)	Error %
(18, 20)	0.55	0.57	3.52
(18, 14)	0.53	0.55	3.65
(15, 14)	0.52	0.53	1.93
(15, 12)	0.48	0.51	5.91
(15, 8)	0.47	0.49	4.08
(15, 6)	0.46	0.48	4.16

Table 1: Shape factor.

References

1. Behera BK, Singh JP (2013) Investigating absorbency behaviour of terry fabric. Res J Text Appal.
2. Behera BK, Singh JP (2014) Objective evaluation of aesthetic characteristics of terry pile structures using image analysis technique. Fibers and Polym 15:2633-2643.
3. Singh JP, Behera BK (2013) Compression behaviour of terry fabric. Proceedings of 13th Autex, Dresden, Germany.
4. Grosberg P (1966) The mechanical properties of woven fabrics part ii: the bending of woven fabrics. Text Res J 36: 205-211.
5. Grosberg P, Swani NM (1966) The mechanical properties of woven fabrics part III: The buckling of woven fabrics. Text Res J 36: 332.
6. Clapp TG, Peng H (1990) Buckling of woven fabrics part I: Effect of fabric weight. Text Res J 60:228-234.
7. Clapp TG, Peng H (1990b) Buckling of woven fabrics part II: effect of fabric weight and frictional couple. Text Res J 60: 285.
8. Ghosh T (1987) Computational model of the bending behaviour of plain woven fabrics. North Carolina State University.
9. Leaf GAV, Anandjiwala RD (1985) A generalized model of plain woven fabric. Text Res J 55: 92-99.
10. Kang TJ, Joo KH, Lee KW (2004) Analyzing fabric buckling based on nonlinear bending properties. Text Res J 74: 172-177.
11. Cornelissen B, Akkerman R(2009) Analysis of yarn bending behaviour.
12. Ivančo V (2006) Nonlinear finite element analysis. University of Applied Sciences-Technology, Business and Design, Wismar.
13. Deshpande S (2010) Buckling and post buckling of structural components.
14. Bao L, Takatera M, Shinohara A (2002) Analysis of large non-linear elastic deformation of fabrics. J Textile Inst 93: 410-419.
15. Zienkiewiez OC, Taylor RL (1991) The finite element method. (4th Ed) McGraw-hill, USA.
16. Hull D, Clyne CW (1996)An Introduction to Composite Materials. (2nd Ed) Cambridge University Press, Cambridge.

17. Sherburn M (2007) Geometric and mechanical modeling of textiles. Nottingham University, USA.

18. Lin H, Sherburn M, Crookston J, Long AC, Clifford MJ, et al. (2008) Finite element modelling of fabric compression. Model and Simul Mater Sci Eng 16: 035010.

19. Yu WR, Kang TJ, Chung K (2000) Drape simulation of woven fabrics by using explicit dynamic analysis. J Textile Inst 91: 285-301.

20. Zhou N, Ghosh TK (1998) On-Line measurement of Fabric bending behaviour. Text Res J 68: 533.